

[illegible]

BY S. ADOLFSSON, A. BAHRAMI, G. BOLMSJÖ AND I. CLAEISSON

WELDING RESEARCH SUPPLEMENT | 59-s



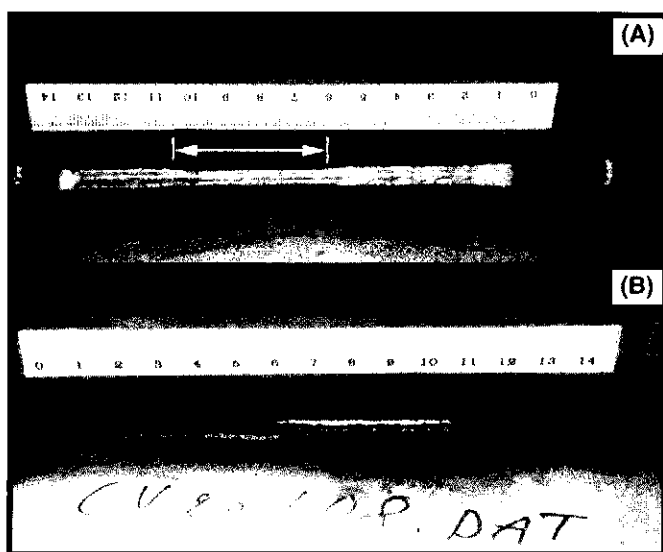


Fig. 5 — T-joint with step disturbance No. 1. Photo of: A — Front; B — rear side of a welded joint. Note that the weld joint at the front of the T-joint in the interval 6–10.5 cm, along the scale (where the weld joint tapers) deviates from normal weld quality, i.e., the size of the leg length and throat dimension is reduced.

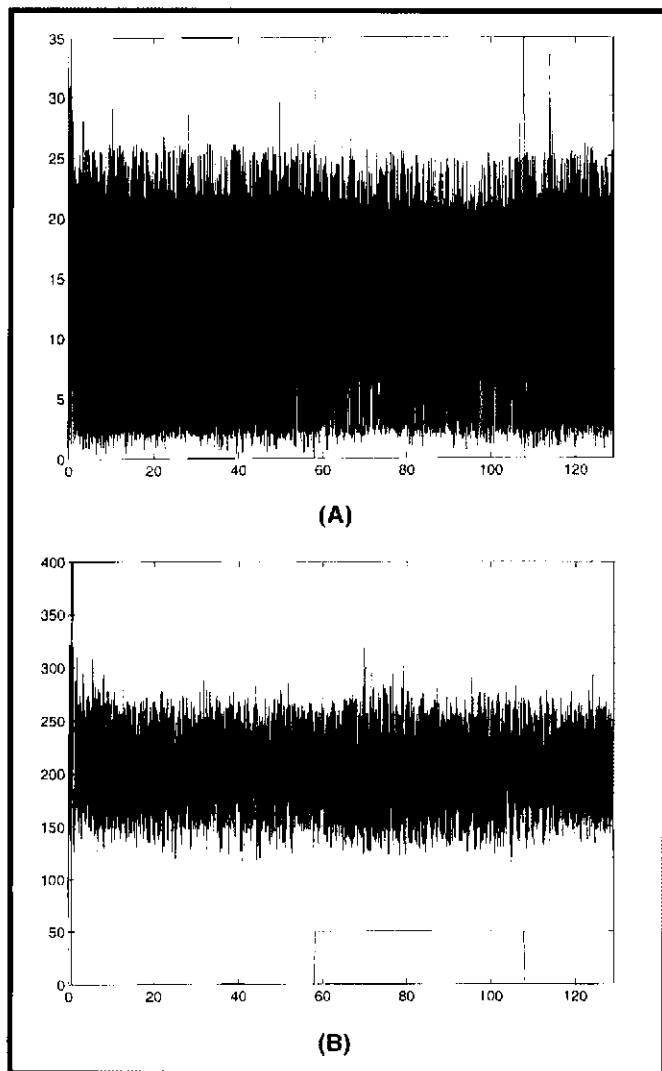


Fig. 6 — T-joint with step disturbance No. 1. A — Measured voltage; B — measured current.

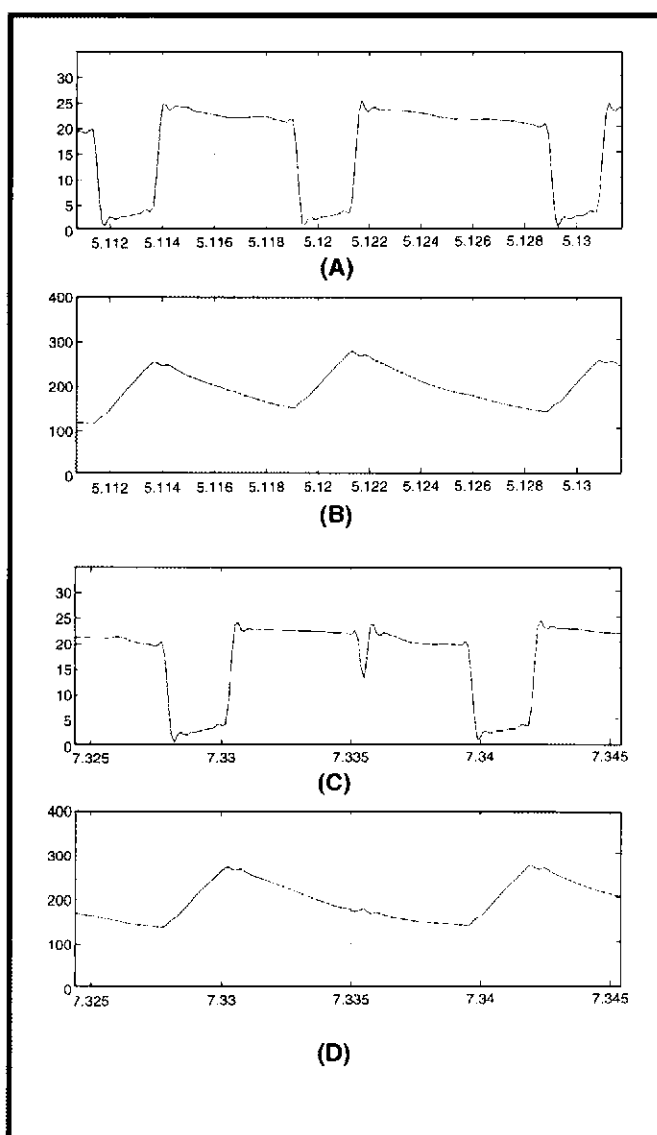


Fig. 7 — Weld voltage and current. Normal weld: A — Measured voltage; B — Measured current. During step disturbance: C — Measured voltage; D — Measured current.

from the electrode wire to the work-piece to be as regular as possible. Experiments have shown that in short-circuit mode, optimal process stability occurs when the short-circuit frequency equals the oscillation frequency of the weld pool (Refs. 5, 6, 20, 21). Optimal process stability corresponds to

- a maximum short-circuit rate (Number/s)
- a minimum standard deviation of the short-circuit rate
- a minimum mass transferred per short-circuit
- a minimum spatter loss.

The welding conditions in which optimal process stability occurs are referred to as *optimal welding conditions*. Deviation from the optimal welding condition is assumed to lead to a higher probability of spatter, uneven weld head and other fusion defects. In this case, the welding process is said to be operating under *non-optimal welding conditions*.

The algorithm discussed in this paper is, however, based on the observation that the

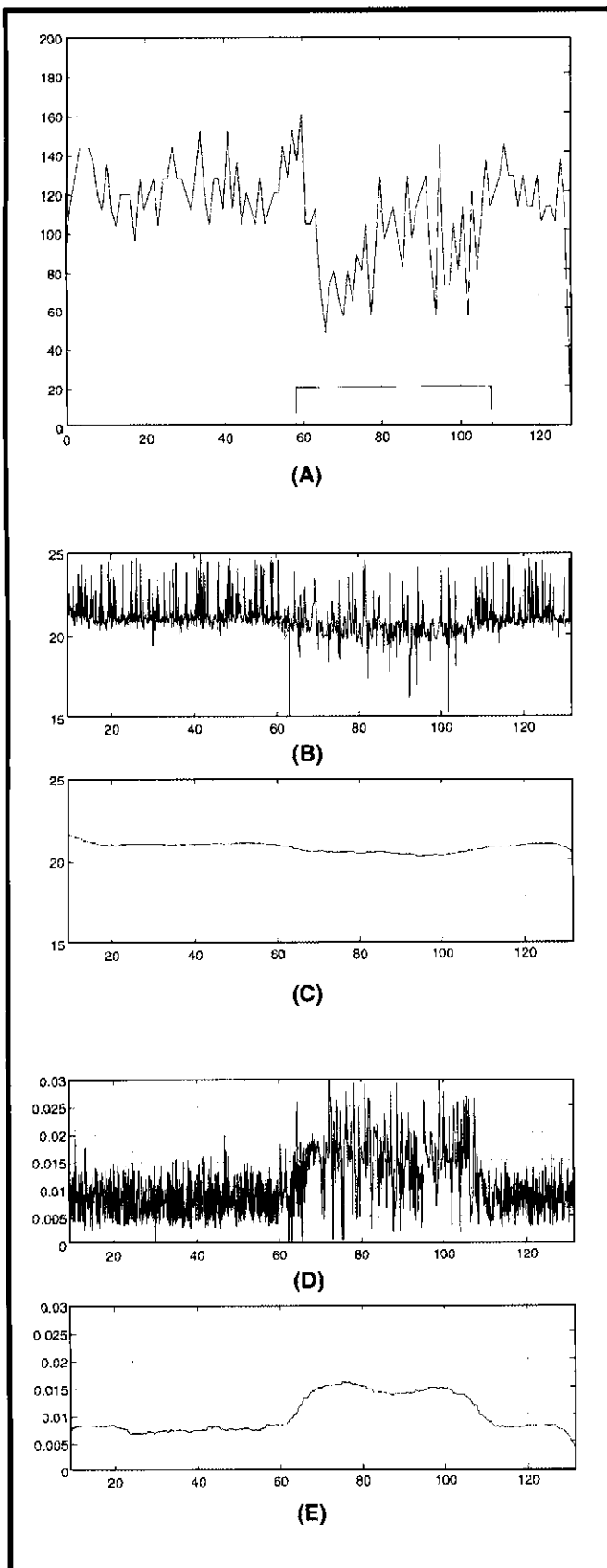


Fig. 8 — T-joint with step disturbance No. 1. A — Measured short-circuit transfer rate; B — estimated mean arc voltage ( $\bar{U}_{wa}$ ); C — median filter of length 100 applied to the estimated mean arc voltage ( $\bar{U}_{wa}^M$ ); D — measured arc time ( $T_a$ ); E — median filter of length 100 applied to the arc time sequence ( $T_a^M$ ).

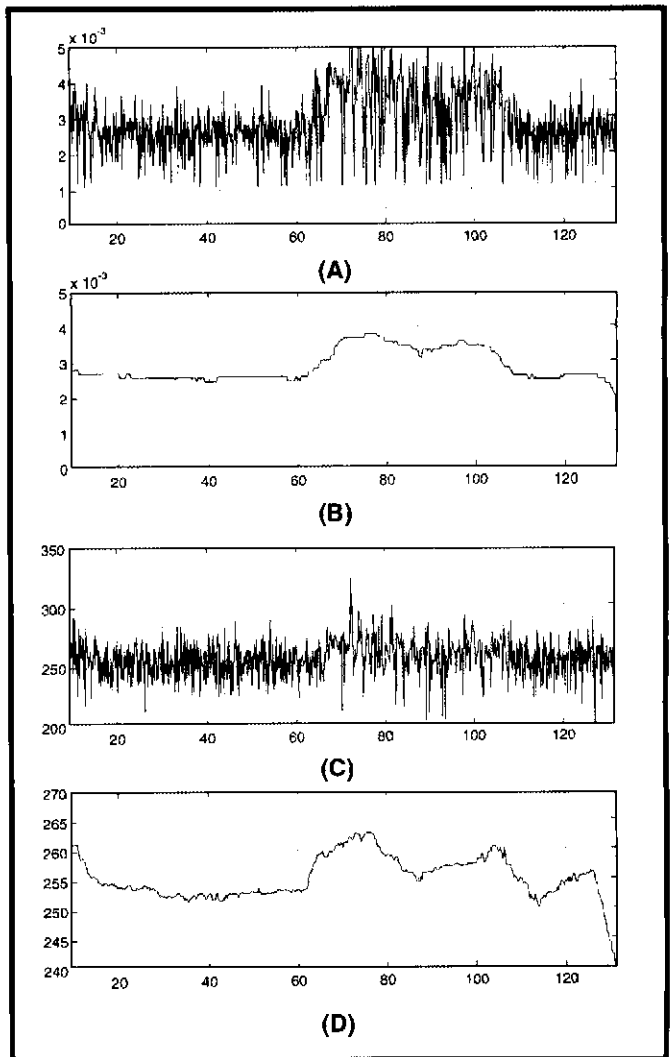


Fig. 9 — T-joint with step disturbance No. 1. A — Measured short-circuit time ( $T_s$ ); B — median filter of length 100 applied to the estimated short-circuit time in part A ( $T_s^M$ ); C — measured short-circuit current peak ( $I_p$ ); D — median filter of length 100 applied to the short-circuit current peak sequence in part C ( $I_p^M$ ).

variance of the weld voltage amplitude decreases when the welding process is not operating under optimal conditions, as shown in Fig. 3 (Refs. 11, 13). It will also be shown below that the arc time, short-circuit rate and standard deviation of the short-circuit rate are less robust parameters than the variance of the weld voltage when detecting defective welds.

## Experiments

### Instrumentation

The experimental setup comprised a welding power source, a Motoman robot carrying a welding torch, a positioner, a welding table and instrumentation for recording weld voltage and current. The work angle of the welding torch was fixed at 45 deg and the travel angle was 0 deg. The distance between the contact tube tip and the plate was 11 mm.

The weld voltage was measured between an electrode applied to the contact tube and a reference electrode screwed into an aluminum plate that served as an insulated welding table (Ref. 14). The current was measured by a current sensor, LEM Module LT 500-S, equipped with a transformer. The sensor was mounted

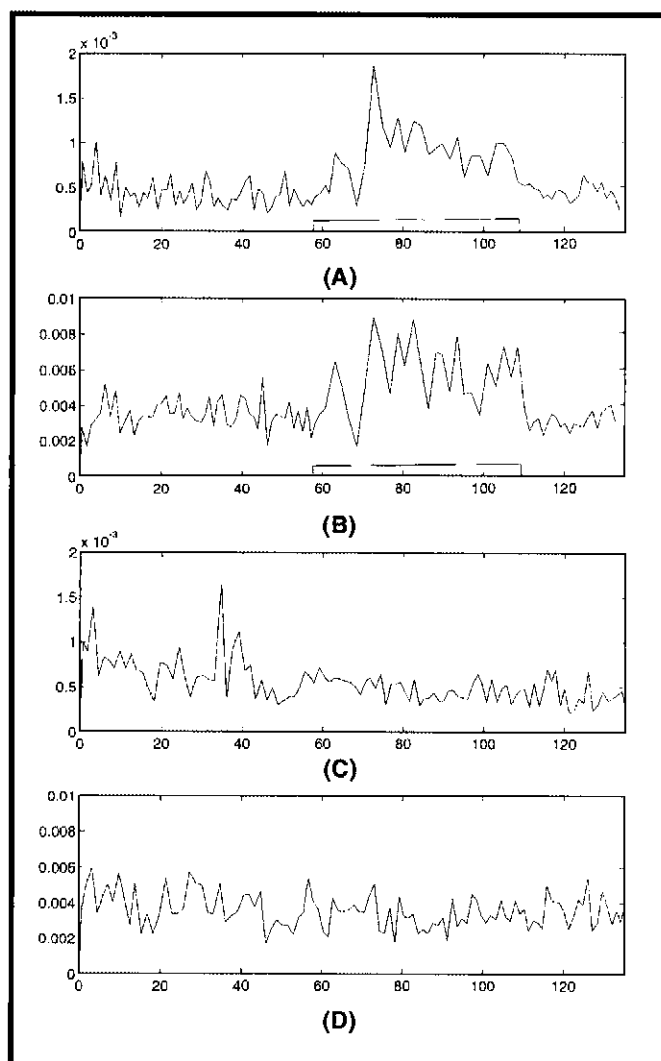
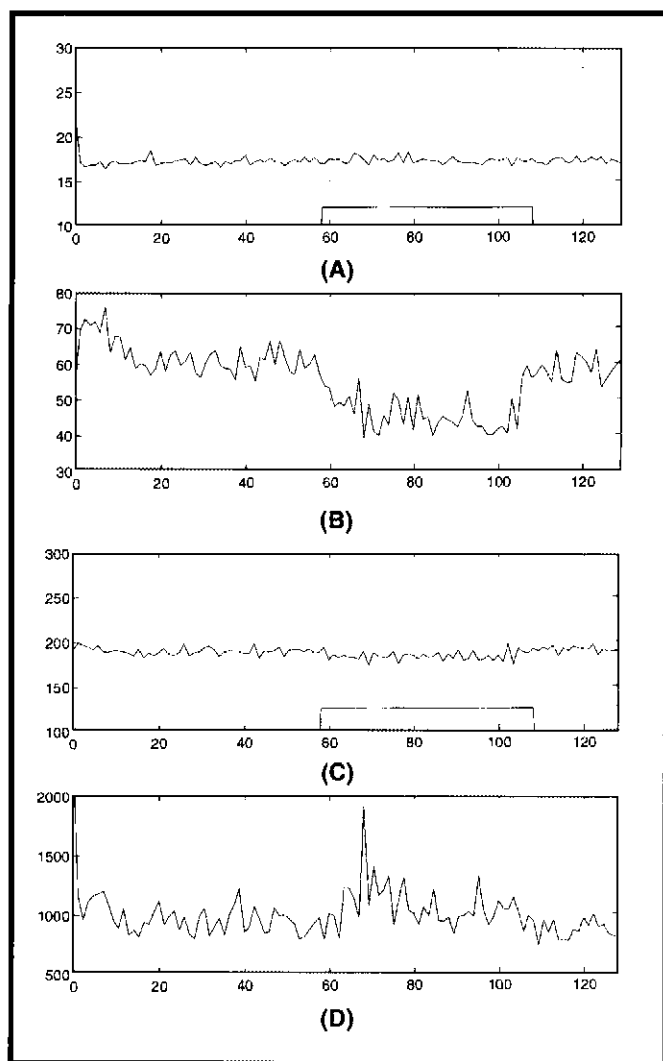


Fig. 10 — T-joint with step disturbance No. 1. A — Mean of the weld voltage ( $m[i]$ ); B — estimated variance of weld voltage ( $y[i]$ ); C — mean of the weld current ( $m[i]$ ); D — estimated variance of weld current ( $y[i]$ ).

Fig. 11 — T-joint with step disturbance No. 1. Standard deviation of: A — Short-circuit time ( $\sigma_s$ ); B — arc time ( $\sigma_a$ ) as a function of position. Reference T-joint. Standard deviation of: C — short circuit time ( $\sigma_s$ ); D — arc time ( $\sigma_a$ ) as a function of position.

around the return conductor. The sampling frequency was 8.192 kHz and the total lowpass filter had a cutoff frequency of 3.0 kHz. The data were transferred for permanent storage to a personal computer.

Two different types of commercial welding equipment, the Migatronik BDH S550 and the Kemppi P500, were used in the experiments. The wire feed rate was measured to be approximately 113–120 mm/s and the nominal welding speed was set at 10 mm/s. The welding wire material used in the experiment was ESAB OK 12.51, with a diameter of 1.0 mm. The shielding gas used was Atal: 80%Ar-20%CO<sub>2</sub>, with a gas flow rate set at 15 l/min.

## Creating Various Welding Conditions

The object of the experiments was to create various welding conditions in a controlled manner, while monitoring the

weld voltage and current from the process — Figs. 4–6. Non-optimal welding conditions were created using a T-joint in which gaps had been cut out from the standing plate — Fig. 4. This specimen was denoted “T-joint with step disturbance.” With the aid of the step disturbance plate, the welding process passed through non-optimal conditions. A second specimen, a T-joint with the standing plate in perfect contact with the laying plate, was used as a reference. This specimen was used to produce normal welds and was denoted “reference T-joint.” During normal welding, the welding process was assumed to be operating under optimal welding conditions.

The specimens comprised two rectangular 200 x 100 x 3-mm plates of SS 1312 mild steel. The dimension of the gap in the T-joint with step disturbance was 2 x

50 mm — Fig. 4C.

A photo of a T-joint with step disturbance is shown in Fig. 5. Note that the weld joint at the front of the T-joint (in the interval 6–10.5 cm along the scale where the weld joint tapers) deviates from normal weld quality, i.e., the size of the leg length and throat dimension is reduced.

## Experimental Data Analysis

### Time Domain Analysis of Measurement Data

The object of this experiment was to confirm, by examination of the waveform of the weld voltage and current, the assumption that the variance of the weld voltage and weld current decreased when the welding process deviated from the optimal welding conditions. Parameters employed in monitoring short arc

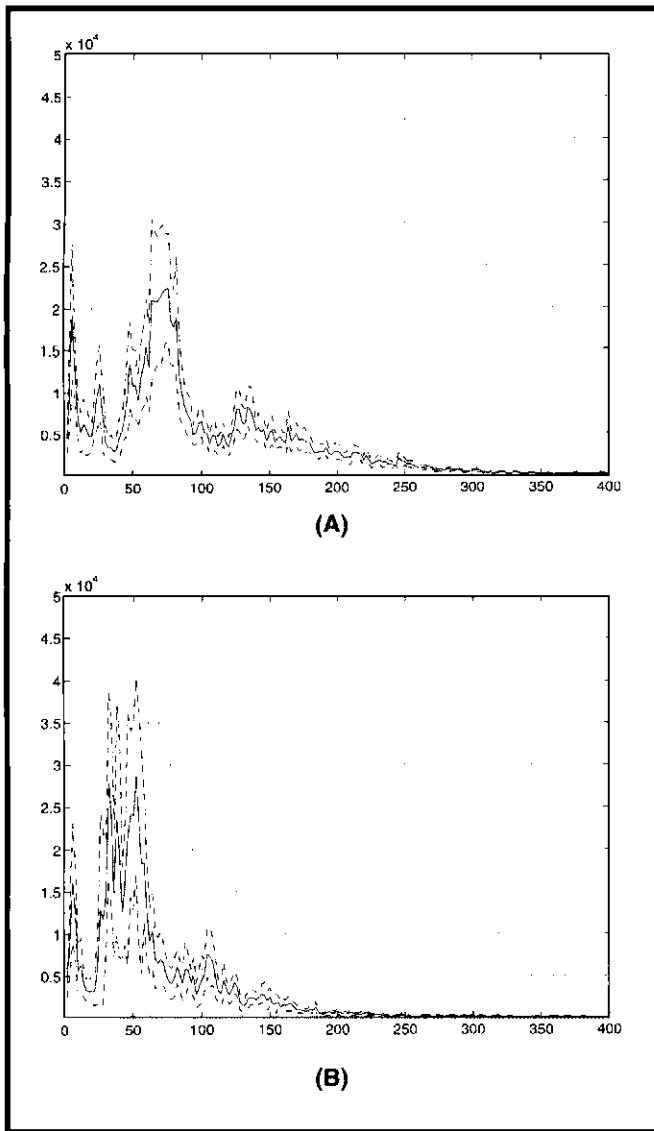


Fig. 12 — Power spectral densities of: A — The weld voltage and weld current from a reference T-joint. Power spectral densities of: B — the weld voltage and weld current during step disturbance. The dotted curve represents 95% confidence limit. Note that the frequency of the spectral maximum peak decreases from about 80 Hz during normal welding to about 50 Hz during step disturbance.

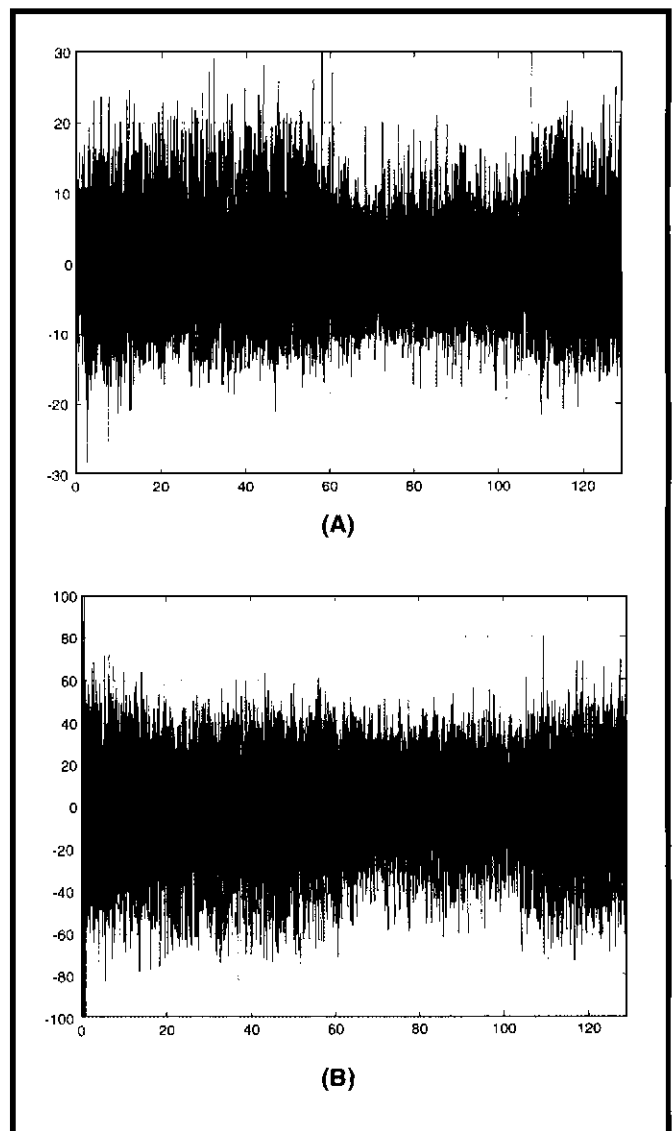


Fig. 13 — Application of high-pass-filter (70 Hz) to: A — Weld voltage; B — current from welding a T-joint with step disturbance. DC and frequency component of the weld voltage and current below 70 Hz is removed and frequency component above 70 Hz is passing through the filter. Note the difference in the waveforms between the non-filtered and the filtered weld voltage and current. (Compare to Fig. 6.)

GMAW were investigated, e.g., arc time,  $T_a$ ; short-circuit time,  $T_s$ ; short-circuit peak current,  $I_p$ ; voltage during arc time,  $U_a$ ; and voltage during short-circuit time,  $U_s$ . These variables are key parameters in GMAW and can be estimated whenever the short-circuit time exceeds 1.0 ms — Figs. 8–11. Note that short-term short-circuits, i.e., those that do not exceed 1.0 ms, can result in non-transference of the molten metal (Refs. 27, 30–32).

The figures that illustrate the estimated short-circuit rate are, however, estimated with the number of short-time short-circuits included. This was done to facilitate visual interpretation of the power spectral diagrams — Fig. 12A–D.

To obtain the overall trend for the estimated features, a sliding median filter of length  $N = 100$  was applied to each parameter sequence. The median filter replaced the center value in the window, with the median value of all samples within the window. For  $N$  even,  $x^M(k)$  is the median of

$$x^M(k) = \text{med} \sum_{n=k-N/2}^{k+N/2-1} x[n]. \quad (2)$$

The output of the median filter is denoted by a superscript  $M$ , e.g., when a median-filter is applied to the arc time,  $T_a$ , the resulting sequence is called  $T_a^M$  — Figs. 8–10.

#### Observation

Two examples of actual recordings of the weld voltages and currents are shown in Fig. 7. Figure 7A and B shows the results of a normal weld; 7C and D show the result of a weld during step disturbance. In Fig. 7A and C, the metal transfers are reflected in the weld voltage as almost zero voltage events of 2 ms. Note that during the step disturbance, the total cycle time,  $T$ , has increased, as compared with a normal weld. The arc time  $T_a$ , short-circuit time  $T_s$  and short-circuit peak current  $I_p$  have also increased during step disturbance welding, as compared with normal welds, while the short-circuit transfer rate and mean

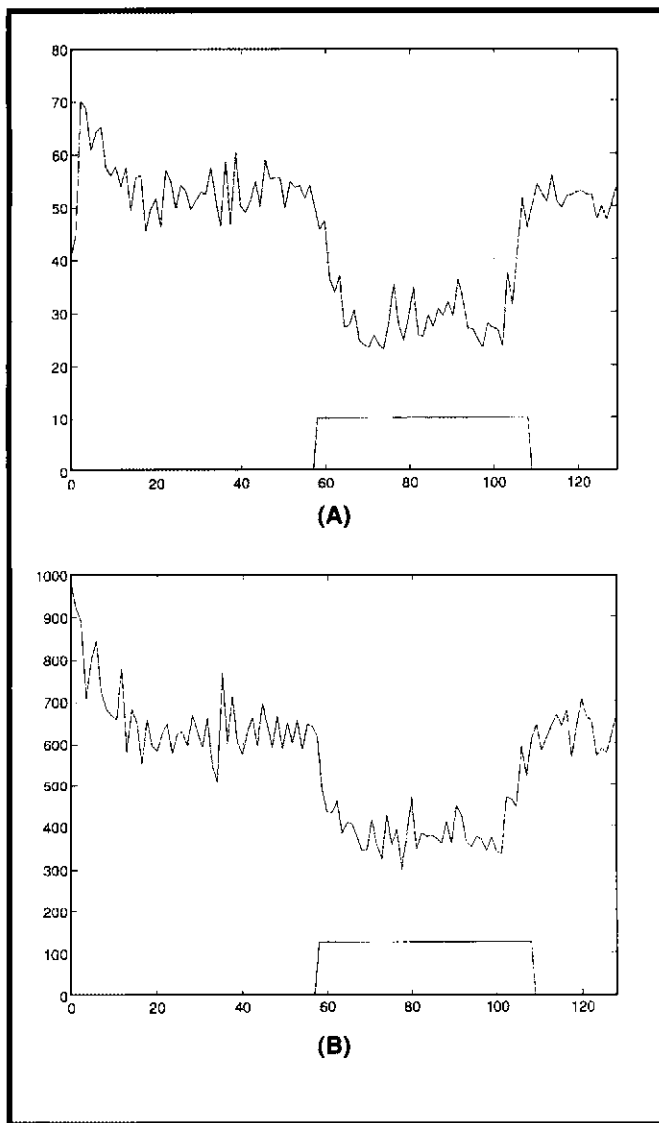


Fig. 14 — Estimated variance of the filtered: A — Weld voltage; B — weld current. Note the similarity in the appearance of the two waveforms. The filtered current shows a decrease in the estimated variance,  $y^2[i]$ , while the non-filtered variance estimate of the weld current,  $y[i]$ , does not decrease during step disturbance. (Compare to Fig. 10D.)

voltage during arc time,  $U_{w,ar}$  have decreased — Figs. 8–10.

A possible physical explanation of these phenomena is as follows: When the weld voltage is too low during arc time, the energy in the arc is not sufficient to melt the electrode and form the droplet that is required to complete the weld cycle — Fig. 8B and C. When this happens, an excessive amount of time must be spent in the short-circuit phase to generate the heat necessary to melt the electrode and release the droplet. Consequently, when the short-circuit time increases, the short-circuit peak current also increases — Fig. 9B and D. These figures also suggest that a larger droplet is detached from the electrode for each short-circuit cycle, to compensate for the decreasing short-circuit metal transfer

rate during step disturbance to balance the wire melting rate with the wire feed rate.

The weld voltage during arc time is approximately 2 V lower than the open circuit voltage (Ref. 33). The exact value is system dependent. Since the weld voltage during arc time decreases during the step disturbance, the welding process is assumed to be operating in the vicinity of A, i.e., the “stubby-in” metal transfer mode in Fig. 3.

#### Mean and Variance of the Weld Voltage and Current

As discussed above, the variance of the weld voltage may be a suitable parameter for detection of changes in the weld quality.

The weld voltage is divided into  $I$  sections, with  $N = 1024$  samples in each section. The variance is calculated for each section and given an index,  $i$ , defined by

the position in the sequence. The variance is estimated as follows:

$$y[i] = \frac{1}{N-1} \sum_{n=(i-1) \cdot N}^{i \cdot N} (u[n] - m[i])^2 \quad (3)$$

$n = 1, 2, \dots, N$   
 $i = 1, 2, \dots, I$

where  $u[n]$  is the weld voltage,  $N$  is the number of data points and  $m[i]$  is the mean of the weld voltage in section  $i$ , calculated as

$$m[i] = \frac{1}{N} \sum_{n=(i-1) \cdot N}^{i \cdot N} u[n] \quad (4)$$

$n = 1, 2, \dots, N$   
 $i = 1, 2, \dots, I$

Figures 10A and B show the result of the estimated mean,  $m[i]$  and variance,  $y[i]$  of the weld voltage amplitude taken from a T-joint with step disturbance.

Calculations of  $m[i]$  and  $y[i]$  of the weld current amplitudes are shown in Fig. 10C and D.

From these diagrams, the following conclusions can be drawn:

1) There is a decrease in the estimated variance of the weld voltage and no change in the mean weld voltage during step disturbance — Fig. 10A and B. This supports the assumption that the short-circuit transfer rate has decreased. Since the short-circuit transfer rate has also decreased, non-optimal welding conditions can therefore be assumed — Figs. 3 and 8A.

2) The variance  $y[i]$  at the beginning of the welding pass is considerable. This is due to the fact that the process is not stabilized, which leads in turn to the numerous high-voltage transients.

3) Unlike the estimated variance of the weld voltage during step disturbance, no decrease in the estimated variance of weld current  $y[i]$  is observed — Fig. 10C.

#### Standard Deviation of Short-Circuit Time and Arc Time

The standard deviations of the arc, short-circuit time, short-circuit peak current and short-circuit frequency have often been used as indicators of the stability and regularity of the welding process (Refs. 4–6, 34, 35).

In this study, only the standard deviation of the arc and short-circuit time were calculated since preliminary results showed that standard deviations in peak current and short-circuit frequency yielded no new information. In other words, the behavior of the standard deviation during step disturbance was approximately identical for the four parameters.

The standard deviation was calculated as follows: Short-circuit time and arc time were divided into sections, with ten observations in each section (ten observations of the short-circuit time and arc time corresponded to a weld joint length of approximately 1.0 mm). The standard deviation was then calculated for each section. The results can be seen in Fig. 11.

#### Spectral Domain Analysis of Measurement Data

Since variance is an AC power estimate (the area below the curve of the power spectral density), spectra from the recordings of normal welding conditions can be compared with spectra of the recordings taken during step disturbance when searching for relevant characteristics (Ref. 36).

The results of the power estimation of







with

$$\lambda[i] = \ln \frac{p_{m1}(y[i])}{p_{m0}(y[i])} \quad (8)$$

to a threshold  $h$ . At the sampling instant  $k$ ,  $\Lambda_j^k$  is computed. If  $\Lambda_j^k \geq h$ , then a defect in the weld joint is detected. In the scalar independent case,  $\Lambda_j^k$  is recursively updated as

$$\Lambda_j^{k+1} = \Lambda_j^k + \lambda[k+1]. \quad (9)$$

In the case of a change in the mean value  $m$  of an independent Gaussian random sequence  $y[i]$  with known variance  $\sigma_f^2$ , the sufficient statistics  $\lambda[i]$  are calculated as (Ref. 22)

$$\lambda[i] = \frac{m_0 - m_1}{\sigma_f^2} \left( \frac{m_0 + m_1}{2} - y[i] \right) \quad (10)$$

which is written as

$$\lambda[i] = \frac{v}{\sigma_f^2} \left( m_0 - y[i] - \frac{v}{2} \right) \quad (11)$$

where

$$v = (m_0 - m_1) \quad (12)$$

is the change in magnitude. The SPRT is optimal with respect to the worst mean delay, when the error probability for false alarms goes to zero. The instant of change  $j$  is, in fact, unknown. This may, however, be estimated using the maximum likelihood principle (Ref. 40), leading to the decision function and alarm instant

$$g[k] = \max_{0 \leq j \leq k} \Lambda_j^k \quad (13)$$

$$t_a = \min\{k : g[k] \geq h\} \quad (14)$$

The algorithm has been formulated as a set of parallel SPRTs, but may equally be viewed as a repeated SPRT or a cumulative sum (CUSUM) type test. The connection between these alternative points of view has been investigated (Ref. 22). The decision function  $g[k]$  introduced in Equation 13 becomes in repeated SPRT formulation

$$g[k] = [g[k-1] + \lambda[k]]^+ \quad (15)$$

and in the Gaussian case

$$g[k] = \left[ g[k-1] + \frac{v}{\sigma_f^2} \left( m_0 - y[k] - \frac{v}{2} \right) \right]^+ \quad (16)$$

where  $(x)^+ = \sup(0, x)$ . The alarm threshold  $h$  is chosen by a tradeoff between worst mean delay time for detection  $\tau$  and false alarm probability  $\alpha$ . The CUSUM algorithm (Ref. 24) is optimal when  $\alpha$  goes to zero:

$$\tau \sim \frac{\ln \alpha^{-1}}{K(m_1, m_0)} \quad \text{when } \alpha \rightarrow 0 \quad (17)$$

where

$$K(m_1, m_0) = E_{m_1} \left[ \ln \frac{p_{m_1}(y[i])}{p_{m_0}(y[i])} \right] \quad (18)$$

is the Kullback information. In the Gaussian case, the Kullback information is

$$K(m_1, m_0) = \frac{(m_1 - m_0)^2}{2 \cdot \sigma_f^2} \quad (19)$$

Due to Wald's equality, the probability of false alarms  $\alpha$  and the alarm threshold  $h$  satisfies following equation:

$$\alpha = e^{-h} \quad (20)$$

when the probability of non-detection goes to zero. The alarm threshold  $h$  is therefore easy to obtain for fixed  $\alpha$  (Ref. 41). The complete fault detection algorithm may be summarized as follows:

For each section  $k$  of 1024 data samples:

- 1) calculate AC power  $y[k]$
- 2) calculate  $g[k] = [g[k-1] + \lambda[k]]$
- 3) if  $g[k] \leq 0$  then  $g[k] = 0$
- 4) if  $g[k] \geq h$  then set Alarm.

#### Estimation of the Mean and Variance of the AC Power Parameter

The AC power of weld voltage  $y[i]$  in Equation 10 is assumed to be identical, independent and Gaussian-distributed, with a mean value  $m_0$  and  $m_1$  under normal and fault welding conditions, respectively. The variance  $\sigma_f^2$  of the AC power is assumed to be constant, during both normal weld and step disturbance. However, the mean and variance of the AC power are not known and must, therefore, be estimated. Since there are both within-record variations (see Fig. 21C) and between-record variations of the AC power (probably due to slightly different welding conditions occurring during the experiments when welding the different T-joints), the between-record variations are incorporated into the total variance  $\sigma_f^2$  — Fig. 20.

To estimate the mean value of the AC power factor, the between- and within-record variance from five experiments (each with 32 observations originating from weld voltages recorded during normal conditions and welds during step disturbance) was used. The process model and estimation procedure of the mean, within-record variations, between-record variations and total variance are described in Ref. 17. The results are given in Table 1. For this data, the mean for normal welds is  $\hat{m}_0 = 56.60$  and during step disturbance,  $\hat{m}_1 = 47.56$ . The estimated variances between record are  $\hat{\sigma}_R^2 = 0.66$  and  $\hat{\sigma}_f^2 = 6.19$ , respectively. The estimated variance within the record for a normal weld is  $\hat{\sigma}_f^2 = 6.26$  and  $\hat{\sigma}_f^2 = 8.84$  during step disturbance. The total variance for the data is  $\hat{\sigma}_f^2 = 6.92$  and  $\hat{\sigma}_f^2 = 14.75$ , respectively.

In the experiment, the total variance  $\sigma_f^2$  was set at 6.92. Due to an underestimation of the total variance during the step disturbance, the worst mean delay time for detection  $\tau$  will increase (Refs. 42, 43).

#### Tuning

In the proposed algorithm, the only tuning parameter is the threshold  $h$  (Table 2). Using Equation 20, we computed the worst mean delay for detection  $\tau$  and chose a false alarm probability  $\alpha$ . These may then be used to determine a relevant alarm threshold,  $h$ .

If the false alarm probability  $\alpha$  is set at  $10^{-6}$  and assuming that the AC power sequence  $y[i]$  is Gaussian and statistically independent, the alarm threshold  $h$  is calculated to be  $h = 13.8$ . The reverse arrangement and the  $\chi^2$  test was applied to the AC power to test whether or not the AC power was Gaussian and statistically independent (Ref. 44). The outcome of these tests — not included in this paper — shows the AC power is likely to be statistically independent, but non-Gaussian during both normal and step disturbance welding (Ref. 17). Since the AC power sequence  $y[i]$  cannot be assumed to be Gaussian, the alarm threshold  $h$  is set at 16 to maintain the false alarm probability,  $\alpha \geq 10^{-6}$ . In real industrial applications, it is recommended that the welder in charge has the option of changing the alarm threshold in accordance with the type of welding mode and application.

#### Test of the Repeated SPRT Algorithm

The recursive SPRT algorithm was tested on 31 specimens. A total of 15 experiments were conducted for reference

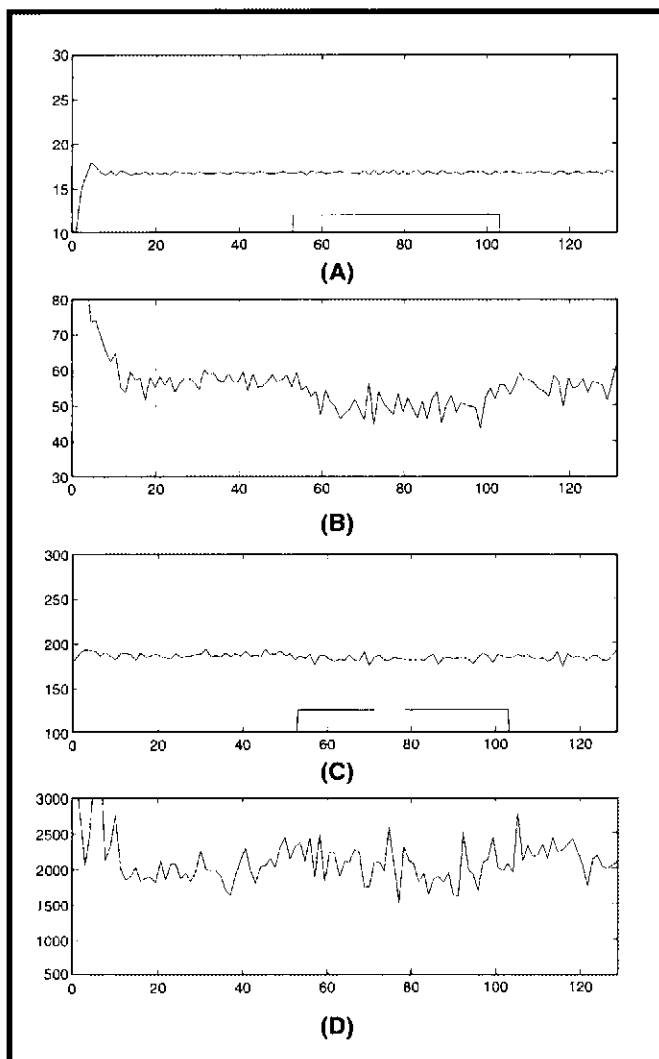


Fig. 17 — T-joint with step disturbance No. 2. A — Mean of the weld voltage ( $m[i]$ ); B — estimated variance of the weld voltage ( $y[i]$ ); C — mean of the weld current ( $mi[i]$ ); D — estimated variance of the weld current ( $yi[i]$ ).

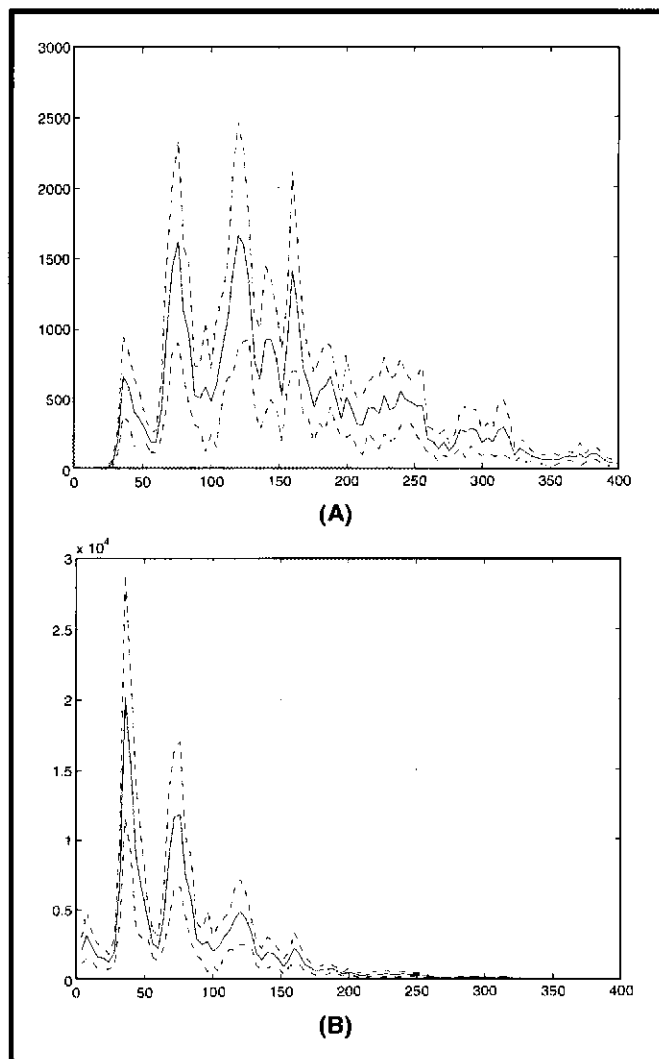


Fig. 19 — T-joint with step disturbance No. 2. Power spectral densities of: A — The weld voltage; B — weld current during step disturbance. The dotted curve represents the 95% confidence limit.

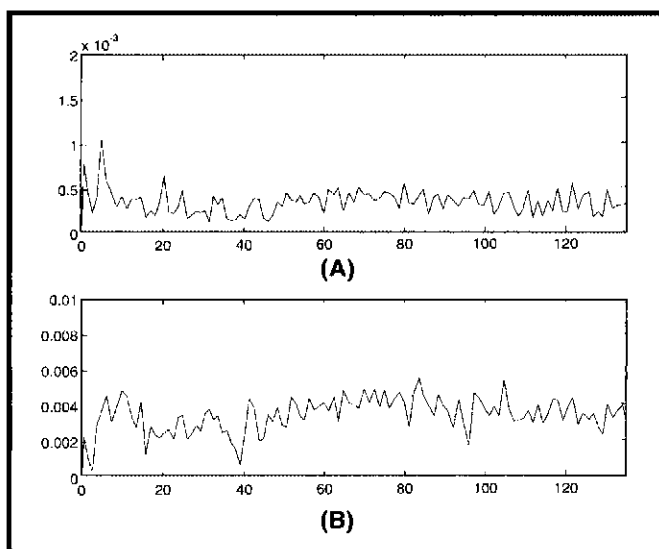


Fig. 18 — T-joint with step disturbance No. 2. Standard deviation of: A — Short-circuit time ( $\sigma_s$ ); B — arc time ( $\sigma_a$ ) as a function of position.

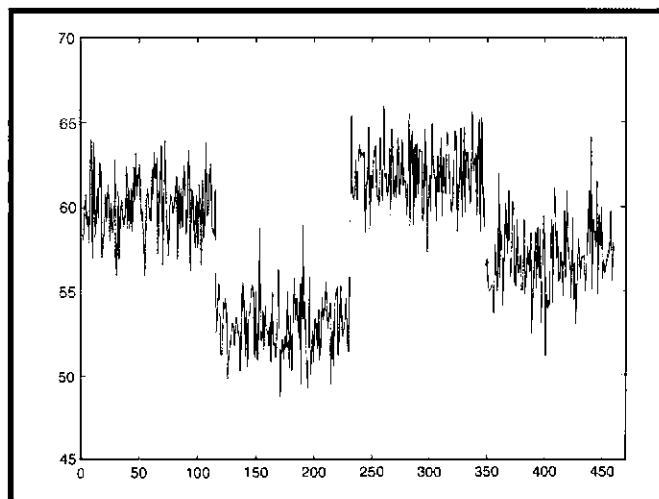


Fig. 20 — The between-record variation of the AC power  $\sigma_R^2$ . This variation is probably due to slightly different welding conditions between the experiments, while the within-record variation  $\sigma_i^2$  is associated with fluctuations along the weld joint during an experiment. The between-record variation is exaggerated in the diagram for illustrative purposes.

**Table 1 — Parameter Estimates During Normal Welds and During Step Disturbance**

Estimated Parameters			
		During Normal Weld	During Step Disturbance
$\hat{\sigma}_T^2$	Estimated within-record variance	6.26	8.84
$\hat{\sigma}_R^2$	Estimated between-record variance	0.66	5.91
$\hat{\sigma}_T^2$	Estimated total variance	6.92	14.75
$\hat{m}$	Estimated overall mean	56.60	47.56

**Table 2 — Design Parameters Selected for the Fault Detection Algorithm for Two Different Values of the Change Magnitude,  $v = 9$  and  $v = 2.63$ , Respectively (Welding Speed is Set at 10 mm/s)**

Design Parameters			
		Test 1	Test 2
$v$	Magnitude of change	9	2.63
$h$	Alarm threshold	16	16
$\alpha$	False alarm probability	$10^{-6}$	$10^{-6}$
$h$	Alarm threshold	16	16
$\sigma_T^2$	Total variance	6.92	6.92
$m_0$	Mean during normal condition	56.60	56.60
$m_1$	Mean during non-optimal condition	47.56	53.97

**Table 3 — The Experimental Results of Test 1 of the SPRT Algorithm (Magnitude of Change  $v$ , is set at 9 and Welding Speed is Set at 10 mm/s)**

Results		
Type of T-Joint	Reference	Step
Number of specimens	15	16
Detection	0	12
Non-detection	0	4
False alarm	0	0

**Table 4 — The Experimental Results of Test 2 of the SPRT Algorithm (Magnitude of Change  $v$  is set at 2.63 and Welding Speed is Set at 10 mm/s)**

Results		
Type of T-Joint	Reference	Step
Number of specimens	15	16
Detection	0	15
Non-detection	0	1
False alarm	0	0

T-joints and 16 experiments were conducted for T-joints with step disturbance. The recording time of the measured signals was 15 s.

The test was designed as follows: When the alarm turns on and there is a step disturbance, the test results in a detection. If the alarm turns on and there is no step disturbance, the result is a false alarm.

Two different changes in magnitude,  $u = m_0 - m_1$  and  $u = 1/2sT$ , were used. The choice of  $u$  was dictated by the experimental results in Table 1. The first choice of  $u$  is the estimated change in magnitude; the second choice is the minimum change in magnitude. The minimum change in magnitude is bound to be positive. It is known, however, that the SPRT algorithm is quicker at detecting a magnitude of change between about  $1/2sT$  and  $3/2sT$  from the target value  $m_0$ , as reflected in the Shewhart chart (Refs. 22, 39, 45).

Since the welding process was not working under optimal welding conditions at the start and end of the welding pass, the alarm was inhibited during the first and last centimeter of the welding pass.

#### Test Results

The results of the test shown in Tables

3 and 4 indicate that it is possible to detect changes in the weld quality automatically and on-line. To illustrate the results of the data, the test result for a T-joint with a step disturbance is shown in Figs. 21 and 22.

#### Discussion

All the tests showed consistent results: during a step disturbance, the AC power of the weld voltage decreased. In the experiments, the decrease in the AC power during step disturbance welding was the same for the two different brands of welding equipment used in the experiments. It is likely, therefore, that other equipment of different brands will also exhibit the same behavior. A suitable change in magnitude  $u$  and target value  $m_0$  must be adjusted for each piece of equipment and for each type of welding.

The proposed SPRT algorithm was designed to detect sudden changes in the average level of the AC power. Four-step disturbances were not detected, however, when the change in magnitude  $v$  was set at 9. These non-detected step disturbances occurred on the same day. A special physical cause could not be found to account for this variation; therefore, these records cannot be excluded from the tests. A probable explanation is that the experimental conditions on the day in question were not identical to the other three. Nevertheless, the recordings from that day all show a decrease in AC power during step disturbance, but the AC power is unusually large — both before as well as during step disturbance. (Compare Figs. 21C and 23.) Since the minimum value that the SPRT algorithm can detect is  $m_0 - u/2$  and the AC power value during step disturbance is above this critical value, these two factors combined explain the lack of detection of the step disturbance.

In industrial welding applications, it is sometimes necessary to weld with mixed-mode transfer to increase the welding speed, thereby increasing productivity. The mix-mode transfer, which contains a mixture of short-circuiting, globular and spray transfer, is related to a working point in the vicinity of C in Fig. 3. In this case, it is relevant to use two SPRT algorithms together: the first for detecting an increase in the mean of the AC power, and the second for detecting a decrease in the mean of the AC power. A new target value  $m_0$ , which corresponds to the new working point, must be estimated together with a robust tuning of the minimum magnitude of change in terms of the Kullback information and of



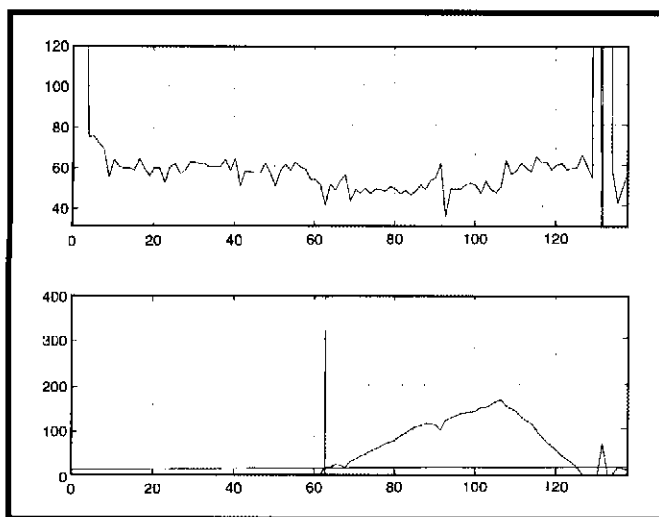


Fig. 24 — An example of the AC power waveform when spatter occurs. High voltage transients give rise to high AC power transients at 13 cm in the diagram.

voltage and current between a normal weld and welds during step disturbance (Ref. 36). The maximum spectral peak during normal welding is about 80 Hz as opposed to the maximum spectral peak during step disturbance, which is approximately 55 Hz. A detection algorithm based on the detection of changes in the fundamental frequencies, together with detection of changes in the amplitude in the fundamental frequencies shows promise. However, preliminary results described above (Ref. 36) have shown that the variance of the weld voltage is the most robust parameter for detecting changes in the weld quality.

#### Acknowledgments

The authors wish to express their gratitude to the Industrial Development Centre of Olofström and its personnel for their support in arranging and assisting with the experimental measurements. We also wish to acknowledge the financial support given by The Foundation for Knowledge and Competence Development (KKS).

#### References

1. Cary, H. B. 1994. *Modern Welding Technology*. Englewood Cliffs, N.J. Regents/Prentice-Hall.
2. Amin, M. 1983. Pulse current parameters for arc stability and controlled metal transfer in arc welding. *Metal Construction* 15(5): 272–278.
3. Cornu, J., and Weston, J. 1995. *Advanced Welding System*, Vol. 2, London, England, IFS.
4. Mite, T., Sakabe, A., and Yokoo, T. 1985. The estimation of arc stability of CO<sub>2</sub> gas shielded arc welding. *Proceedings of the*

Welding Institute Conference: *Advanced Welding Systems*, pp. 261–271.

5. Gupta, S. R., Gupta, P. C., and Rehfeldt, D. 1988. Process stability and spatter generation during dip transfer in MAG welding. *Welding Review*, pp. 232–241.

6. Hermans, M. J. M., and den Ouden, G. 1997. A stability criterion for short circuiting gas metal arc welding. *Proceedings of the International Conference on the Joining of Materials*, Helsingør, pp. 112–119.

7. Jennings, C. 1951. Dynamic characteristics of DC welding machines. *Welding Journal* 30(2): 117–138.

8. Popkov, A., et al. 1977. Reducing the spatter of liquid metal in CO<sub>2</sub> welding by means of optimisation of the welding parameters. *Welding Production* 3: 26–27.

9. Leino, K., Nikkola, A., and Vartiainen, K. 1984. Prediction of weld defects using welding condition data. Research report 264, Technical Research Center of Finland.

10. Adam, G., and Siewert, T. A. 1990. Sensing of GMAW droplet transfer modes using an ER 100S-I electrode. *Welding Journal* 69(3): 103–108.

11. Johnson, J. A., Carlson, N. M., Smartt, H. B., and Clark, D. E. 1991. Process control of GMAW: Sensing of metal transfer mode. *Welding Journal* 70(4): 91–99.

12. Wang, W., Liu, S., and Jones, J. E. 1995. Flux cored arc welding: Arc signals, processing and metal transfer characterization. *Welding Journal* 74(11): 369–377.

13. Ogunbiyi, B., and Norrish, A. 1996. GMAW metal transfer and arc stability assessment using monitoring indices. *Proceedings of the 6th International Conference on Computer Technology in Welding*, TWI, Cambridge, England, Abington Publishing.

14. Adolfsson, S., Ericson, K., and Agren, B. 1995. On automatic detection of burn-through in GMA welding — weld voltage analysis. Research report TULEA 1995:15, Sweden, Division of Signal Processing, Luleå University of Technology.

15. Adolfsson, S., Ericson, K., and Grennberg, A. 1996. Automatic detection of burn-through in GMA welding using a parametric model. *Mechanical Systems and Signal Processing* 10(5): 633–651.

16. Adolfsson, S., Bahrami, A., and Claesson, I. 1996. Quality monitoring in robotised welding using sequential probability ratio test. *Proceedings of TENCO '96, Digital Signal Processing Applications*, Vol. 2, New York, N.Y., IEEE, pp. 635–640.

17. Adolfsson, S., Bahrami, A., Bolmsjö, G., and Claesson, I. 1997. Automatic quality

monitoring in robotised GMA welding using a repeated sequential probability ratio test method. *International Journal for the Joining of Materials* 9(1): 2–8.

18. Blakeley, P. J. 1992. Developments in monitoring systems for resistance and arc welding. *Proceedings of the International Conference on Automated Welding Systems in Manufacturing*, Paper 40. Gateshead, England, Woodhead Publishing, Ltd.

19. Agren, B. 1995. Sensor integration for robotic arc welding. Ph.D. thesis, Sweden, Lund University.

20. Hermans, M. J. M., Spikes, M. P., and den Ouden, G. 1993. Characteristic features of the short circuiting arc welding process. *Welding Review International* 12(2): 80–86.

21. Rehfeldt, D., and Schmitz, T. 1995. Investigation and measurement of weld pool oscillation in GMAW. Technical report, IIW-doc. 212-882-95.

22. Basseville, M., and Nikiforov, I.V. 1993. *Detection of Abrupt Changes: Theory and Application*. Englewood Cliffs, N.J., Prentice-Hall.

23. Grainger, R. W., Hoist, J., Isaksson, A. J., and Ninness, B. M. 1994. A parametric statistical approach to fdi for the industrial actuator benchmark. Research report LUTFD2/TFMS — 3106 — SE LUTFD2/TFMS-3106-SE, Sweden, Dept. of Mathematical Statistics, Lund Institute of Technology.

24. Lorden, G. 1971. Procedures for reacting to a change in distribution. *Ann. Math. Statistics* 42: 1897–1908.

25. Allum, C. J. 1985. Metal transfer in arc welding as a varicose instability: I. Varicose instabilities in a current-carrying liquid cylinder with surface charge. *British Journal of Applied Physics* 18(7): 1447–1468.

26. Amin, M. 1981. Synergic pulse MIG welding. *Metal Construction* 13(6): 349–353.

27. Smith, A. A. 1966. Characteristics of the short-circuiting CO<sub>2</sub>-shielded arc. *Physics of the Welding Arc*, Institute of Welding, pp. 75–91.

28. Lancaster, J. F., ed. 1986. *The Physics of Welding*. Oxford, England, Pergamon Press.

29. Kim, J. A., and Eager, N. M. 1991. Analysis of metal transfer in gas metal arc welding. *Welding Journal* 70(6): 91–99.

30. Mita, T., Sakabe, A., and Yokoo, T. 1988. Quantitative estimates of arc stability for CO<sub>2</sub> gas shielded arc welding. *Welding International* 12(2): 152–159.

31. Piuchuk, I. S., et al. 1980. Stabilization of transfer and methods of reducing the spatter of metal in CO<sub>2</sub> welding with short arc. *Automatic Welding* 6.

32. Shinoda, T., Nishikawa, H., and Shimizu, T. 1996. The development of data processing algorithms and assessment of arc stability as affected by the titanium content of GMAW wires during metal transfer. *Proceedings of the 6th International Conference on Computer Technology in Welding*, TWI, Cambridge, England, Abington Publishing.

33. Lundin, R., and Widfeldt, M. 1988. *Mätning, registrering och övervakning av svetsdata*. Technical report 264, IVF.

34. Liu, S., and Siewert, T. 1989. Metal transfer in gas metal arc welding: droplet rate. *Welding Journal* 68(2): 52–58.

35. Lucas, W. 1985. Computers in arc welding — the next industrial revolution, part 3: instrumentation and process analysis. *Metal Construction* 17(7): 431–436.

36. Adolfsson, S., Bahrami, A., Bolmsjö, G., and Claesson, I. 1997. Quality monitoring in robotized short circuiting GMA welding. Research report HK-R 1997:3, Sweden, Department of Signal Processing, University of Karlskrona/Ronneby.

37. Oppenheim, A. V., and Schaffer, R. W. 1989. *Discrete-Time Signal Processing*. Englewood Cliffs, N.J., Prentice-Hall.

38. Papouis, A. 1984. *Probability, Random Variables, and Stochastic Processes*. New York, N.Y., McGraw-Hill.

39. Montgomery, D. C. 1985. *Introduction to Statistical Quality Control*. New York, N.Y., J. Wiley & Sons.

40. Rao, C. R. 1973. *Linear Statistical Inference and Its Applications*. New York, N.Y., Wiley & Sons.

41. Wald, A. 1947. *Sequential Analysis*. New York, N.Y., J. Wiley & Sons.

42. Bagshaw, M., and Johnson, R. A. 1975. The effect of serial correlation on the performance of CUSUM-tests part II. *Technometrics* 17(1): 73–80.

43. Bagshaw, M., and Johnson, R. A. 1975. The influence of reference values and estimated variance on the ARL of the CUSUM tests. *Jal Royal Statistics Society*, 37(B) (3): 413–420.

44. Bendat, J. S., and Piersol, A. G. 1986. *Random Data: Analysis and Measurement Procedures*. New York, N.Y., J. Wiley & Sons.

45. Wetherill, G. B., and Brown, D. W. 1991. *Statistical Process Control*. England, Chapman and Hall, London.

## List of Symbols

$\alpha$  False alarm probability  
 $f_s$  Sampling rate (Hz)  
 $g[i]$  Decision function  
 $h$  Threshold for alarm  
 $i, j, k, l, m, n$  Integers  
 $I$  Total number of sections within a record  
 $I$  Source current (A)

$I_p$  Short-circuit peak current (A)  
 $j$  Record index, instant of change  
 $K(m_1, m_0)$  Kullback information  
 $\lambda[k]$  Increment of  $\Lambda_k^i$   
 $\Lambda_j^k$  Log-likelihood ratio for observation from  $y[j]$  until  $y[k]$   
 $L_i$  Internal inductance of the power source (H)  
 $l_a$  Length of arc (mm)  
 $l_e$  Length of wire electrode stickout (mm)  
 $m$  Overall mean for the AC power  
 $m[i]$  Mean value, weld voltage, section  $i$  (V)  
 $m_R$  Mean value, AC power, weld voltage, record  $r$   
 $m_0$  Mean value, AC power, weld voltage, normal weld  
 $m_1$  Mean value, AC power, weld voltage, step disturbance  
 $N(0, 1)$  Normal distribution function with zero mean and unit variance  
 $P_{AC}[i]$  AC power of the weld voltage of section  $i$   
 $P_{AC}[r, i]$  AC power of the weld voltage of the section  $i$  of the record  $r$   
 $\Delta P_{AC} R[r]$  Variation between the records  
 $\Delta P_{AC} I[r, i]$  Variation within the record  
 $p_\theta(y|i)$  Probability density function  
 $R$  Total number of records  
 $R_i$  Internal resistance of the power source ( $\Omega$ )  
 $\sigma_a$  Standard variation of the arc time  
 $\sigma_A^2$  Variance of total number of reverse arrangements, A  
 $\sigma_f^2$  Within-record variance of the AC power  
 $\hat{\sigma}_f^2$  Estimated within-record variance of the AC Power

$\sigma_R^2$  Between-record variance of AC power  
 $\hat{\sigma}_R^2$  Estimated between-record Variance of AC power  
 $\sigma_s$  Standard variation of the short circuit time  
 $\sigma_f^2$  Total variance,  $\sigma_W^2 + \sigma_\beta^2$ , of the AC power  $P_{AC}[r, i]$   
 $\hat{\sigma}_f^2$  Estimated total variance  $e, \hat{\sigma}_W^2 + \hat{\sigma}_\beta^2$ , of the AC power  $P_{AC}[r, i]$   
 $t_a$  Alarm instant  
 $T$  Total cycle time,  $T = T_a + T_{sh}$  (s)  
 $T_a$  Arc time (s)  
 $T_s$  Short-circuit time (s)  
 $\tau$  Mean delay time for detection  
 $\theta_0$  Parameter before change  
 $\theta_1$  Parameter after change  
 $u[n]$  Weld voltage at the sampling instant (V)  
 $U_a$  Arc voltage (V)  
 $U_e$  Wire electrode stickout voltage (V)  
 $U_{oc}$  Open circuit voltage (V)  
 $U_p$  Peak voltage (V)  
 $U_w$  Weld voltage,  $U_w = U_e + U_a$  (V)  
 $U_{wa}$  Weld voltage during arc time (V)  
 $U_{ws}$  Weld voltage during short-circuit time (V)  
 $v$  Change magnitude  
 $W_b$  Wire melting rate (mm/s)  
 $W_f$  Wire feed rate (mm/s)  
 $W_s$  Welding speed (mm/s)  
 $y[i]$  Variance, weld voltage, section  $i$   
 $y[i]$  AC power, weld voltage, section  $i$